Chromatography **2015**, *2*, 625-641; doi:10.3390/chromatography2040625

OPEN ACCESS

chromatography

ISSN 2227-9075

www.mdpi.com/journal/chromatography

Article

Prediction of Peak Shape and Characterization of Column Performance in Liquid Chromatography as a Function of Flow Rate

Juan José Baeza-Baeza, Casandra Ortiz-Bolsico and María Celia García-Alvarez-Coque *

Departament de Química Analítica, Universitat de València, c/Dr. Moliner 50, 46100 Burjassot, Spain

* Author to whom correspondence should be addressed; E-Mail: celia.garcia@uv.es.

Academic Editor: Frank L. Dorman

Received: 24 August 2015 / Accepted: 29 September 2015 / Published: 2 November 2015

Abstract: Traditionally, column performance in liquid chromatography has been studied using information from the elution of probe compounds at different flow rates through van Deemter plots, which relate the column plate height to the linear mobile phase velocity. A more recent approach to characterize columns is the representation of the peak widths (or the right and left peak half-widths) for a set of compounds *versus* their retention times, which, for isocratic elution, give rise to almost linear plots. In previous work, these plots have been shown to facilitate the prediction of peak profiles (width and asymmetry) with optimization purposes. In this work, a detailed study on the dependence of the peak widths (or half-widths) on the flow rate is reported. A new approach to quantify the deterioration of column performance for slow and fast flow rates and to characterize chromatographic columns is proposed. The approach makes use of the width (or half-widths) for a set of compounds with similar interaction kinetics and does not require knowledge of the extra-column contributions to the total variance. The chromatographic data of two sets of compounds of different natures (sulfonamides and β-blockers), eluted from Spherisorb and Chromolith columns with acetonitrile-water mixtures, are used to illustrate the approach.

Keywords: liquid chromatography; width plots; flow rate; prediction of peak profiles; column characterization

---

1. Introduction

Band broadening in liquid chromatography depends on several processes that take place inside the column: the multiple pathways that a solute can travel through the column packing, molecular diffusion and convection in the mobile phase, slow mass transfer kinetics between the stationary and mobile phases, besides extra-column effects [1,2]. A particular concern is the behavior of protonated basic compounds analyzed using alkyl-bonded silica-based columns, for which the retention and peak profile are significantly affected by slow adsorption-desorption equilibria between the cationic species and the free silanols buried by the alkyl chains, giving rise to significant peak broadening and asymmetry [3,4].

The overall performance of a chromatographic system, expressed as the observed peak variance, σ^2_{tot}, has two contributions:

$$\sigma^2_{\text{tot}} = \sigma^2_{\text{col}} + \sigma^2_{\text{ext}} \tag{1}$$

where σ^2_{col} is the column variance that accounts for the dispersion mechanisms inside the column and σ^2_{ext} accounts for the extra-column contribution (from the connecting tubing, column end fittings, frits, injection plug, detector cell and other sources of dispersion in the chromatographic system external to the column) [5–8].

A common practice to determine the column performance is quantifying the height equivalent to a theoretical plate, *H*, which, according to the Martin and Synge plate model, is calculated as follows [9]:

$$H = \frac{L}{N} = \frac{\sigma^2_{\text{col}}}{t^2_{\text{col}}} L \tag{2}$$

where *L* is the column length, *N* the total number of column theoretical plates (plate count or efficiency) and t_{col} is the time the solute needs to go through the column in isocratic conditions. From Equations (1) and (2):

$$H = \frac{\sigma^2_{\text{tot}} - \sigma^2_{\text{ext}}}{(t_{\text{R}} - t_{\text{ext}})^2} L \tag{3}$$

where t_{col} is expressed as the difference between the retention time (t_{R}) and the extra-column contribution to the retention (t_{ext}). The requirement of measuring the extra-column contribution to the total variance is a drawback of the application of this approach, owing to the uncertainty in this measurement. In fact, *H* varies significantly with the flow rate depending on the retention time of the compound used in the measurements. On the other hand, this approach is based on the theoretical plate model, which assumes Gaussian peaks for sufficiently large efficiencies [10]. However, peaks are usually tailing [11–14], and in some cases, they are fronting [15]. Even in these cases, Equation (3) is applied, using numerical integration to obtain the retention times and variances.

For non-Gaussian peaks, the representation of the left and right half-widths at fixed flow rate instead of the variance, *versus* the retention time, offers additional information about the peak profiles [7,16–18]. Although the plots are slightly parabolic inside large retention time ranges, they are linear within practical ranges:

$$A = m_A t_R + n_A \quad (4)$$

$$B = m_B t_R + n_B \quad (5)$$

where A and B are the left and right half-widths of chromatographic peaks in time units, respectively, m_A and m_B the slopes of the linear representations and n_A and n_B the corresponding intercepts. The slopes in Equations (4) and (5) are dimensionless, since A, B and t_R are all measured in the same time units. A similar plot can be obtained for the widths ($w = A + B$):

$$w = m_w t_R + n_w \quad (6)$$

m_w and n_w being the corresponding slope and intercept.

Equations (4) to (6) have been demonstrated to be useful to predict peak profiles with optimization purposes, to characterize chromatographic columns and to reveal the interaction kinetics of solutes [17]. The model parameters in these equations can be obtained by fitting the half-widths (or widths) *versus* the retention times for a set of solutes with similar interaction kinetics, eluted with a mobile phase at fixed composition or with mobile phases of different compositions. When the solutes experience different kinetics, the model parameters will be solute dependent and should be obtained for each solute using mobile phases of variable composition (in order to obtain data at different retention times). Recently, the half-width (width) plots approach has been adapted to gradient elution [18,19].

Traditionally, column characterization in liquid chromatography is performed through the elution of probe compounds at different flow rates by representing van Deemter plots [2,20], which relate H for a given solute, column and mobile phase composition to the linear mobile phase velocity. This approach operates with two peak parameters (retention and variance) for the intra- and extra-column effects, which could lead to data affected by significant uncertainty due to the propagation of random errors. In this work, an alternative approach is proposed based on the dependence of the half-widths (or widths) on the flow rate, which increases the reliability of the data, since the experimental peak profile parameters of several compounds and/or conditions are used, and there is no need to measure the extra-column contribution to the retention. The chromatographic data of two sets of compounds of different natures, sulfonamides and β-blockers, isocratically eluted from Spherisorb and Chromolith columns with acetonitrile-water mixtures, are used to illustrate the approach.

2. Experimental Section

2.1. Reagents and Columns

The sulfonamides, sulfamerazine, sulfamethizole, sulfachloropyridazine, sulfisoxazole and sulfadimethoxine (Sigma, St. Louis, MO, USA), and the β-blockers, atenolol, acebutolol, propranolol (Sigma), esmolol (Du Pont-De Nemours, Le Grand Saconnex, Switzerland) and oxprenolol (Ciba-Geigy, Barcelona, Spain), were used as probe compounds. All compounds were dissolved with a small amount of acetonitrile and diluted with water to reach the concentration of the injected solutions (approximately 10 μg/mL).

In all cases, the mobile phases were prepared with HPLC-grade acetonitrile from Scharlau (Barcelona) and buffered at pH 3 using 0.01 M sodium dihydrogen phosphate from Panreac (Barcelona) and HCl from Scharlau. Nanopure water obtained with a Barnstead purification system

from Sybron (Boston, MA, USA) was used throughout. The mobile phases and the probe compound solutions were filtered through 0.45-μm nylon membranes with a diameter of 47 mm (Magna) and 17 mm (Cameo), respectively, from Osmonics (Herentals, Belgium).

The separations were carried out with the following columns: Spherisorb C_{18} (150 mm × 4.6 mm ID, 5-μm particle size) from Scharlab (Barcelona) and Chromolith SpeedROD C_{18} (50 mm × 4.6 mm ID) from Merck (Darmstadt, Germany).

2.2. Apparatus and Measurement of Peak Parameters

The chromatographic system was equipped with the following modules from Agilent (Waldbronn, Germany): quaternary pump, automatic sampler, temperature controller and UV-visible detector (Series 1200 and 1260). The column temperature was set at 25 °C and the signals monitored at 254 and 225 nm for sulfonamides and β-blockers, respectively. The chromatographic system was controlled by an OpenLAB CDS LC ChemStation from Agilent (B.04.03).

The flow rate ranged between 0.2 and 2 mL/min for the Spherisorb column and between 0.2 and 2 mL/min or 0.125 and 5 mL/min for the Chromolith column. The dead time was measured with a solution containing 20 μg/mL of uracil from Acros Organics (Geel, Belgium).

The half-widths were measured at 10% peak height. This allowed an adequate characterization of the asymmetry not affected by the baseline noise of the chromatograms. The half-widths and retention times of chromatographic peaks were measured with the MICHROM software [21]. Data treatment was implemented in an Excel spreadsheet from Microsoft (Seattle, WA, USA).

3. Results and Discussion

3.1. Prediction of Retention Time and Peak Profile at Varying Flow Rates

Both the retention time and peak profile are affected by the flow rate. Therefore, this factor (alone or used with other factors) can be useful to optimize the elution conditions to get appropriate analysis time and resolution. For this purpose, accurate predictions of both retention time and half-widths are needed to reproduce the chromatographic peaks using appropriate peak functions [22,23] and to quantify peak overlapping as a function of flow rate [24]. As known, the retention time exhibits a linear variation with the inverse flow rate ($1/F$):

$$t_R = \frac{d_1}{F} + d_0 \quad (7)$$

Accordingly, accurate linear fittings of t_R *versus* $1/F$ were obtained for all cases examined in this work, with determination coefficients $R^2 > 0.9999$. Therefore, Equation (7) can be used to predict the retention at several flow rate values, with mean prediction errors below 0.5%.

The prediction of half-widths (or widths for symmetrical peaks) is also fundamental for the optimization of a chromatographic separation, as this allows the accurate quantification of the overlapping between adjacent peaks. In Figure 1, the left and right half-widths for the sets of sulfonamides (Figure 1a,b) and β-blockers (Figure 1c,d), analyzed with the Spherisorb column, are represented against the retention time at fixed (Figure 1a,c) and variable (Figure 1b,d) flow rates. At a fixed flow rate, the behavior is linear (*i.e.*, the trends in Equations (4) and (5) are followed) for both

sets of compounds. In contrast, when the retention times change as a consequence of the flow rate, the behavior is parabolic (*i.e.*, the slope changes), since the efficiency changes: at high and low flow rates, the half-widths are larger than expected, considering the optimal linear behavior. For sulfonamides, the peaks are almost symmetrical, and consequently, the plots for the right and left half-widths practically agree, whereas for β-blockers, the peaks are significantly tailing. Therefore, the slope of the plot for the right half-width is larger. In this case, the flow effects are hidden by the general deterioration of the efficiency.

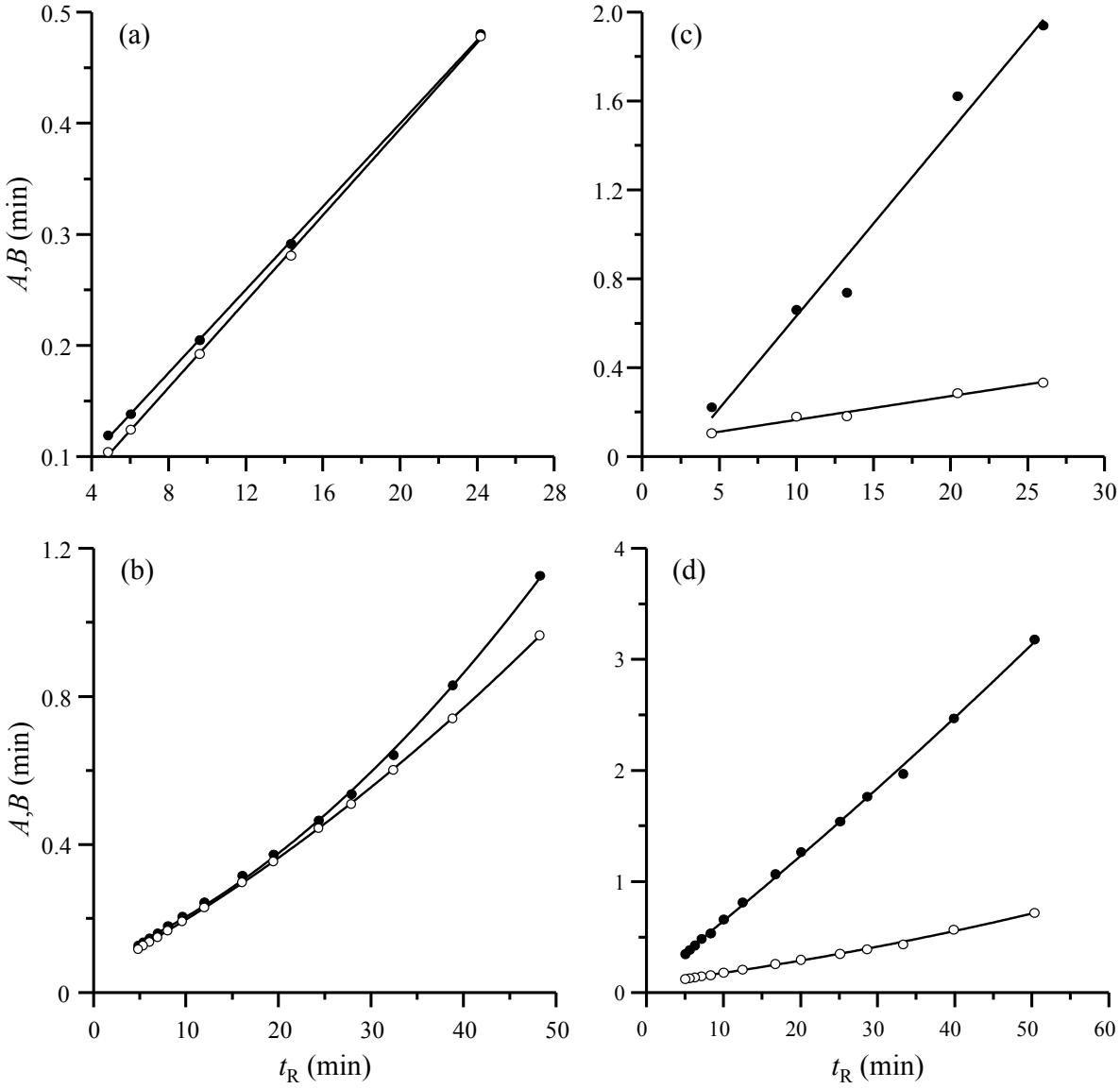

Figure 1. Peak half-width plots for the sets of sulfonamides (**a**,**b**) and β-blockers (**c**,**d**), eluted from the Spherisorb column. Half-widths correspond to: (**a**,**c**) five compounds eluted at 1 mL/min and (**b**) sulfachloropyridazine and (**d**) acebutolol eluted at variable flow rates in the range 0.2 to 2 mL/min. Mobile phase: 20% v/v acetonitrile for sulfonamides, and 65% v/v for β-blockers. Left (*A*, ○) and right (*B*, ●) half-widths.

In Figure 2, the dependence of the left half-widths (A) *versus* the inverse flow rate is shown for the set of five sulfonamides and the dead time marker. In all cases, the half-widths fit a parabola:

$$A = \frac{b_2}{F^2} + \frac{a_2}{F} + c_2 \quad (8)$$

where a_2, b_2 and c_2 are model parameters. Equation (8) (and a similar equation for the right half-width, B, and for the width, w) allows a simple prediction of the half-widths at any flow rate in the measured range, with errors below 0.6% for the right half-width and below 2.0% for the left half-width for the solutes under study (the determination coefficients were always $R^2 > 0.9998$). As observed in Figure 2, the half-widths depend on the retention behavior of each compound. Consequently, particular models should be fitted.

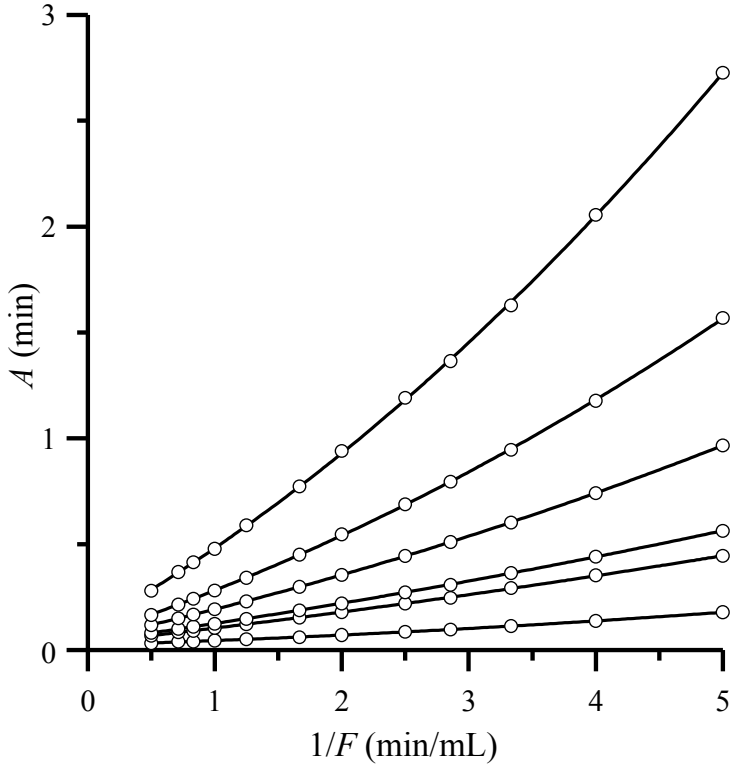

Figure 2. Dependence of the left (A) half-width with the inverse flow rate, for the set of sulfonamides and the dead time marker (uracil), analyzed using the Spherisorb column and 20% v/v acetonitrile. From top to bottom: sulfamerazine, sulfamethizole, sulfachloropyridazine, sulfisoxazole, sulfadimethoxine and uracil. Similar plots can be obtained for the right half-width and the width.

3.2. Characterization of the Column Performance Based on the Peak Half-Widths

Next, it is shown how the performance of chromatographic columns can be described based on the dependence of the slopes for the representation of the right and left half-width plots (m_A and m_B in Equations (4) and (5)) or a similar plot for the width (m_W in Equation (6)) *versus* the flow rate. For this purpose, we propose three approaches, for which a separate measurement of the extra-column contribution is not needed, since this would only affect the intercept of the plots.

3.2.1. Approach I

In Figure 3a,b, the slopes in Equations (4) and (5) are represented as a function of the flow rate and compared to the change in height equivalent to a theoretical plate, calculated according to Equation (2), for the same dataset (Figure 3c). Similar trends are obtained for both half-widths and theoretical plates: the behavior of the slopes for the peak half-width and width plots can be thus described using an equation of the same type as the theoretical plates. For the left half-width:

$$m_A = a + \frac{b}{F} + cF \tag{9}$$

and similarly for the right half-width (B) and the width (w). The parameters a, b and c in Equation (9) can be useful to characterize a chromatographic column. Note that these parameters do not have the same physical meaning as the parameters in the van Deemter equation. However, the practical application of the new approach and its interpretation is very simple, since m_A in Equation (4) (and similar parameters for the right half-width and the width) indicates the peak broadening increment per unit time inside the column.

Therefore, the parameters in Equation (9) can be used to measure the column performance. Parameter a is the contribution to the peak broadening independent of the flow rate. It describes the vertical shift of the curves in Figure 3a,b and can be explained based on equilibrium considerations, convection and eddy diffusion. Parameter b is the contribution explained by factors that increase at decreasing flow rate, as the diffusion. Finally, parameter c is the contribution explained by factors that increase at increasing flow rate, as the slow mass transfer.

Parameters a, b and c in Equation (9) can be obtained in two steps. First, the peak half-widths (or widths) for a set of compounds eluted at fixed, or at varying mobile phase composition, or for a single compound eluted at varying mobile phase compositions are linearly fitted *versus* the retention times, in order to obtain m_A (or similar parameters for the right half-width and width). In the second step, the slopes obtained at several flow rates are non-linearly correlated with the flow rate according to Equation (9).

3.2.2. Approach II

The parabolic behavior depicted in Figure 2 *versus* the flow rate (described by Equation (8)) and the trend for the slope of the half-width (or width) plots described in Equation (9) suggest that the independent term in Equations (4) to (6) (n_A, n_B and n_w) should also follow a parabolic trend, as was corroborated. Considering also Equation (7), with $d_0 = 0$ and $d_1 = V_R$, the behavior can be modelled as follows:

$$A = \left(a + \frac{b}{F} + cF \right) \frac{V_R}{F} + \frac{b_0}{F^2} + \frac{a_0}{F} + c_0 \tag{10}$$

from which:

$$A = (b V_R + b_0) \frac{1}{F^2} + (a V_R + a_0) \frac{1}{F} + (c V_R + c_0) = \frac{b_2}{F^2} + \frac{a_2}{F} + c_2 \tag{11}$$

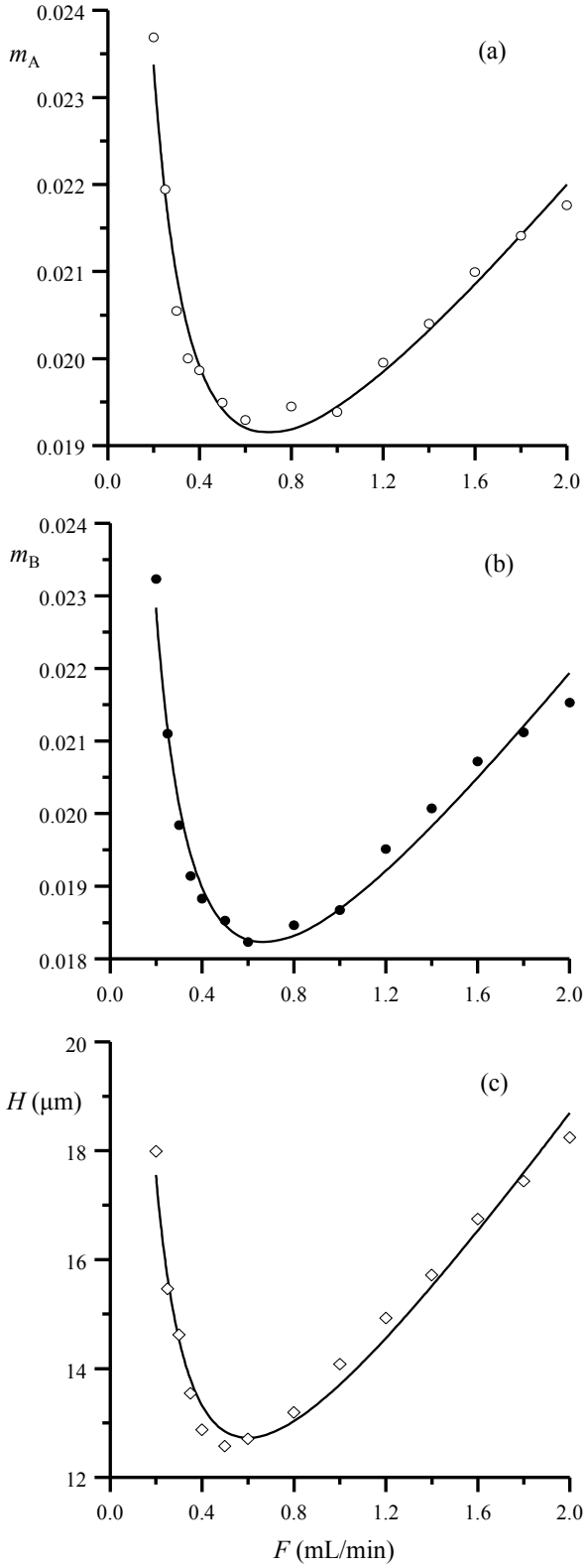

Figure 3. Representation *versus* the flow rate of the slopes of the linear fittings of: (**a**) the left and (**b**) right half-width/retention time data (Equations (4) and (5), respectively) for the set of five sulfonamides and (**c**) height equivalent to a theoretical plate for sulfamerazine, calculated using Equation (3). The plotted data were obtained with a Spherisorb column and 20% v/v acetonitrile. The lines in the plots correspond to the non-linear fittings to Equation (9) (or similar).

Equation (11) and similar ones indicate that the coefficients of the parabolic relationship of the half-widths (or widths) with the inverse flow rate are linearly related to the retention volumes, as shown in Figure 4 for the Spherisorb column. This gives rise to a second approach. In the first step, the half-widths (or width) for each probe compound in the set are fitted against the flow rate according to Equation (8). In the second step, the a_2, b_2 and c_2 coefficients for the different compounds are linearly correlated with their retention volume (see Equation (11) and Figure 4). The slopes of the fitted straight lines are the model parameters a, b and c in Equation (9).

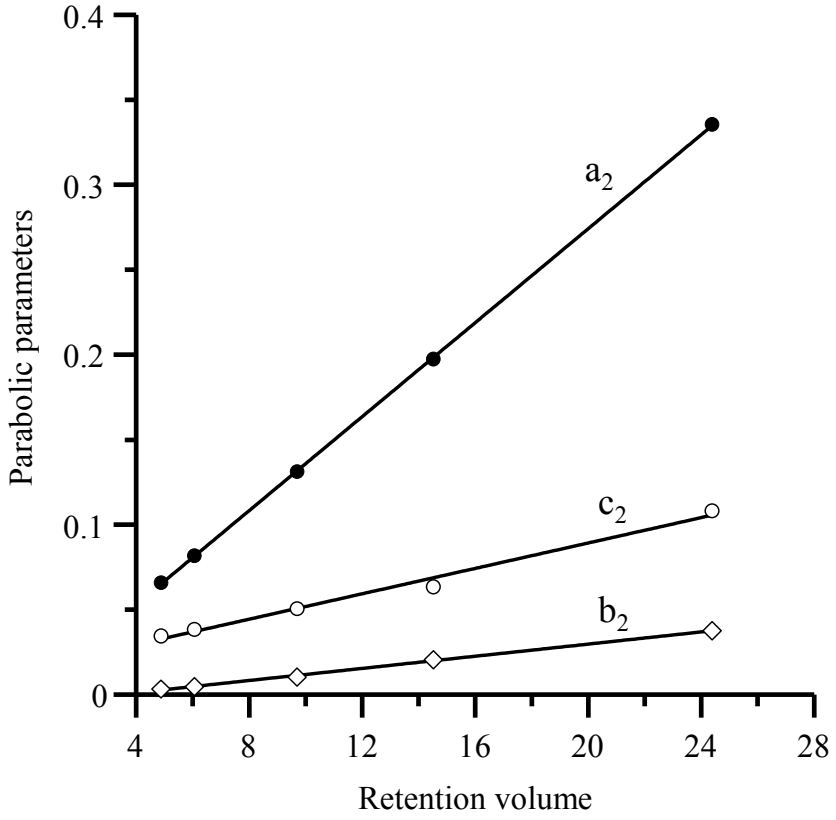

Figure 4. Representation of parameters a_2, b_2 and c_2 in Equation (11) *versus* the retention volume (V_R) for the five sulfonamides. The plotted parameters were obtained in the fitting of the left half-widths for each sulfonamide eluted with the Spherisorb column at different flow rates (see Figure 1).

3.2.3. Approach III

Equation (10) can be taken as the basis for a third approach to obtain the model parameters a, b and c in a single step, where the half-widths of several compounds at several flow rates are non-linearly fitted *versus* the flow rate. In order to avoid overweighting in the least-squares fitting of the data at the lowest flow rates (and consequently, at the highest retention times), the half-widths should be better expressed in volume units:

$$A_V = A \times F = \left(a + \frac{b}{F} + c\,F \right) V_R + a_0 + \frac{b_0}{F} + c_0\,F \tag{12}$$

where V_R is calculated as the product $t_R \times F$.

3.3. Characterization of the Spherisorb and Chromolith Columns

In Table 1, the model parameters in Equation (9) (obtained according to the three approaches described above) are compared for the set of sulfonamides. The results from Approaches I and III are similar. Approach III is the most practical, since all data are fitted in a single step. By applying the Excel Solver tool, fitting of the data took only a few seconds. However, Approach I has the interest of showing in detail the behavior of the half-widths (or widths) with time and flow rate. Approach II is less reliable due to the flexibility of the parabolic fitting, with parameters more strongly affected by random errors.

Table 1. Model parameters in Equation (9) (or a similar equation for the right half-width), according to the three approaches, for the Spherisorb and Chromolith columns using the set of sulfonamides as probe compounds [a].

	Left half-width (*A*)				**Right half-width (*B*)**			
	a	***b***	***c***	**ε_r (%)**	***a***	***b***	***c***	**ε_r (%)**
Spherisorb column								
Approach I	0.0144	0.00166	0.00338	1.5	0.0126	0.00188	0.00420	1.6
Approach II	0.0138	0.00179	0.00373	1.1	0.0118	0.00206	0.00467	1.4
Approach III	0.0144	0.00166	0.00339	1.3	0.0125	0.00188	0.00420	1.6
Chromolith column								
Approach I	0.0340	0.00364	0.00267	2.1	0.0248	0.00525	0.00524	3.4
Approach II	0.0355	0.00342	0.00221	4.4	0.0270	0.00490	0.00444	3.2
Approach III	0.0340	0.00364	0.00268	2.1	0.0247	0.00525	0.00527	3.1

[a] Mean relative prediction errors were calculated according to $\varepsilon_r(\%) = \left(\sum|y_i - \hat{y}_i|\right)/\left(\sum|y_i|\right)\times 100$, where y_i and $\hat{y}_i$ are the experimental and predicted data, respectively.

The model parameters in Equation (9) for the sets of sulfonamides and β-blockers, separated with the Spherisorb and Chromolith columns, are compared in Table 2. Note that, as expected, the model parameters for the peak width agreed with the sum of the parameters for the left and right half-widths. The poorer fittings for the β-blockers should be explained by the differences in the interaction kinetics among these compounds with the silanols on the stationary phases. However, the information given by the model parameters is still useful and shows the large differences in the model parameters between both half-widths. However, note that the proposed approaches cannot be applied to sets of data where the compounds exhibit more different kinetics.

For sulfonamides, parameters *a* and *b* are smaller for the Spherisorb column, partially due to the longer length. The Chromolith column offers similar behavior at increasing flow rate (*c* parameter) for these compounds. For β-blockers, the right half-widths are more affected by the flow rate. From the parameters obtained with the data of sulfonamides and β-blockers, it is evident that the interaction behavior is different for both sets of compounds (especially for the Spherisorb column), with the largest differences associated with parameter *a*.

Table 2. Model parameters according to Approach III for the Spherisorb and Chromolith columns, using the set of sulfonamides and β-blockers as probe compounds [a].

Parameter	*a*	*b*	*c*	R^2	ε_r (%)
Spherisorb column/sulfonamides					
A	0.0144	0.00166	0.00339	0.9993	1.3
B	0.0126	0.00188	0.00420	0.9987	1.6
w	0.0270	0.00354	0.00759	0.9990	1.4
Chromolith column/sulfonamides					
A	0.0340	0.00364	0.00268	0.9987	2.1
B	0.0247	0.00525	0.00527	0.9976	3.1
w	0.0587	0.00889	0.00795	0.9983	2.4
Spherisorb column/β-blockers					
A	0.00650	0.00125	0.00330	0.967	6.2
B	0.0821	0.00116	−0.00084	0.974	8.2
w	0.0886	0.00241	0.00246	0.975	7.6
Chromolith column/β-blockers					
A	0.0268	0.00182	0.00163	0.986	5.3
B	0.0888	0.00067	0.00860	0.983	7.2
w	0.1156	0.00248	0.01022	0.989	5.7

[a] Fitting determination coefficients (R^2) and accuracy (measured as mean relative prediction errors) are given (see Table 1 for more details).

3.4. Optimal Flow Rate

If the extra-column effects are neglected, the optimal flow rate (F_{opt}) corresponding to the minimal band broadening inside the column can be obtained from Equation (9), as follows:

$$-\frac{b}{F_{opt}^2} + c = 0 \tag{13}$$

For the set of sulfonamides eluted with the Spherisorb column, $F_{opt} = \sqrt{b/c}$ = 0.70 mL/min. If the extra-column broadening is included, the optimal flow rate should be obtained from Equation (11):

$$F_{opt} = \sqrt{\frac{b_2}{c_2}} = \sqrt{\frac{bV_R + b_0}{cV_R + c_0}} \tag{14}$$

which means that the optimal flow rate will depend on the analyzed compound. Taking the parameters given in Table 3 for each compound, the optimal flow rate ranged between F_{opt} = 0.31 for sulfamerazine and F_{opt} = 0.59 for sulfadimethoxine. Only for sufficiently high retention, the optimal flow rate would tend to 0.70. This means that there is no single optimal flow rate for all compounds and suggests that the application of a flow rate gradient would give rise to the best peak profile for each compound. It should be however observed that most applications use higher flow rates than the optimal, due to practical reasons.

Table 3. Retention factor and model parameters for the left half-width for sulfonamides [a].

	k	***a***	***b***	***c***
Sulfamerazine	3.16	0.0135	0.00067	0.00714
Sulfamethizole	4.20	0.0135	0.00077	0.00626
Sulfachloropyridazine	7.26	0.0137	0.00103	0.00520
Sulfisoxazole	11.35	0.0139	0.00135	0.00429
Sulfadimethoxine	19.79	0.0142	0.00143	0.00416
Set of five sulfonamides	–	0.0144	0.00166	0.00339

[a] Parameters a, b and c correspond to Equation (12), assuming $a_0 = b_0 = c_0 = 0$.

The geometrical interpretation of the optimal flow rate is depicted in Figure 5 for sulfamerazine. The half-widths measured in volume units ($A \times F$) are represented *versus* the flow rate in Figure 5a. It may be observed that in this plot, the changes in the half-widths with respect to the optimal value (the minimum indicating the optimal flow rate) are accentuated. In contrast, the representation of A in time units *versus* $1/F$ depicts a parabolic behavior, where the loss of linearity is only remarkable at low flow rates, corresponding to the loss of efficiency due to the diffusion (Figure 5b). The optimal flow rate corresponds to the point where the slope of the parabola matches the straight line that goes through the origin (*i.e.*, the parabola tangent). From Equations (8) and (11):

$$\frac{dA}{d(1/F)} = \frac{2b_2}{F_{op}} + a_2 = \frac{A}{1/F} = \frac{b_2}{F_{op}} + a_2 + c_2 F_{op} \tag{15}$$

which yields:

$$\frac{b_2}{F_{op}} = c_2 F_{op} \tag{16}$$

This result agrees with Equation (14). Finally, representing $A \times F^2$ *versus* the flow rate (Figure 5c), a parabola is also obtained, where the effect of high flow rates is highlighted.

The extra-column effects are isolated in Equation (10) through the a_0, b_0 and c_0 terms. Therefore, the a, b and c terms refer only to the chromatographic column. In Table 3, the column parameters for the whole set of sulfonamides eluted from the Spherisorb column are compared to the parameters fitted for each sulfonamide, making $a_0 = b_0 = c_0 = 0$ in Equation (12), which implies that the extra-column effects are included inside the parameters a, b and c as in Equation (11). As observed, as the solute retention increases, these parameters tend to those obtained with the data for the whole set of compounds, since the extra-column effects are less important.

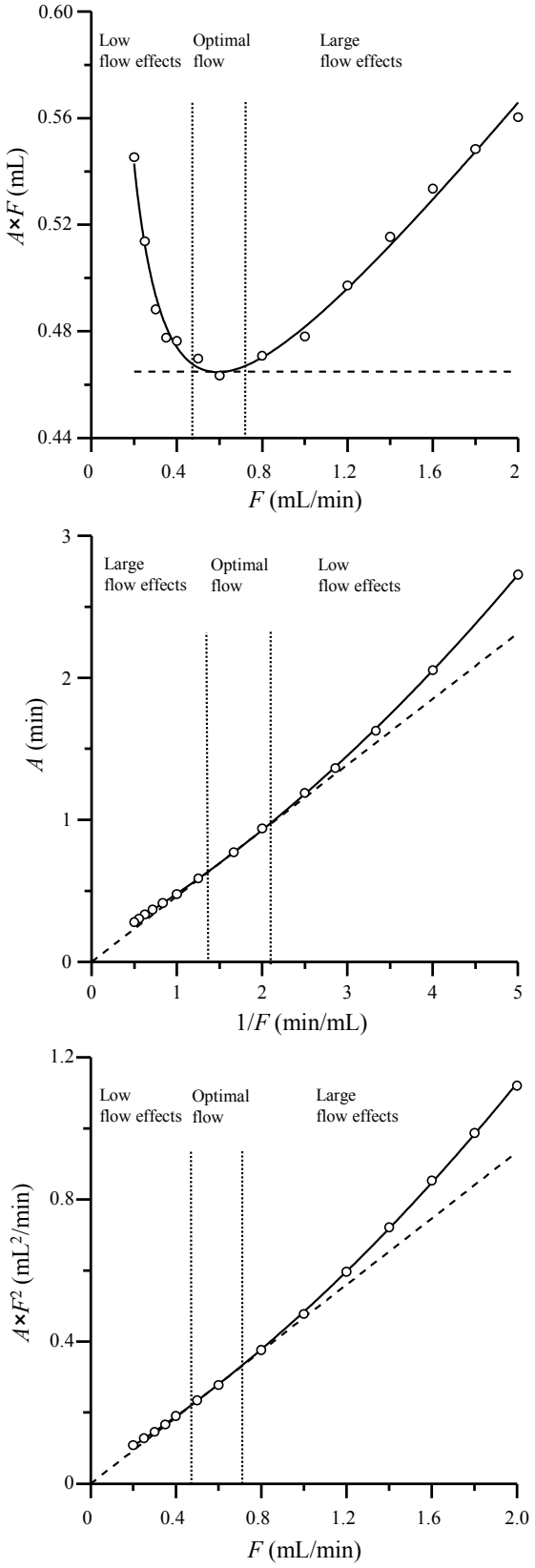

Figure 5. Dependence of the left half-width and derived parameters on the flow rate (or inverse flow rate), for sulfisoxazole, showing the region of optimal elution. In each diagram, the intersection with the dashed straight lines indicates the optimal elution. The deviations from these lines can be explained by diffusion and slow mass transfer processes.

3.5. Peak Capacity

The study of column performance can be enriched by evaluating the dependence on the flow rate of the column peak capacity (P_c), which is the maximal number of adjacent peaks located at exactly the right distance to yield enough resolution in a certain time window. The calculation of the peak capacity with the proposed approach, as a function of the peak half-widths, is rather simple:

$$P_c = 1 + \frac{1}{1.4(m_A + m_B)} \ln\left(\frac{(m_A + m_B)V_n + n_A + n_B}{(m_A + m_B)V_1 + n_A + n_B}\right) \quad (17)$$

Equation (17) has been adapted to volume units from Equation (50) in [25], to account for the peak compression when time units are used due to the flow. In the equation, V_1 and V_n are the extreme volumes of the range where the peak capacity is calculated. In Figure 6, the experimental and predicted peak capacities for the set of sulfonamides eluted in a Spherisorb column at varying flow rates are depicted. The experimental P_c is calculated from the *m* and *n* values (slope and intercept) for the linear fittings of the half-widths in volume units *versus* the elution volume, using equations similar to Equations (4) and (5). The predicted peak capacities are calculated using Approach III and Equation (12) to obtain the *m* and *n* values from the fitted parameters (*a*, *b*, *c*) and (a_0, b_0, c_0), respectively.

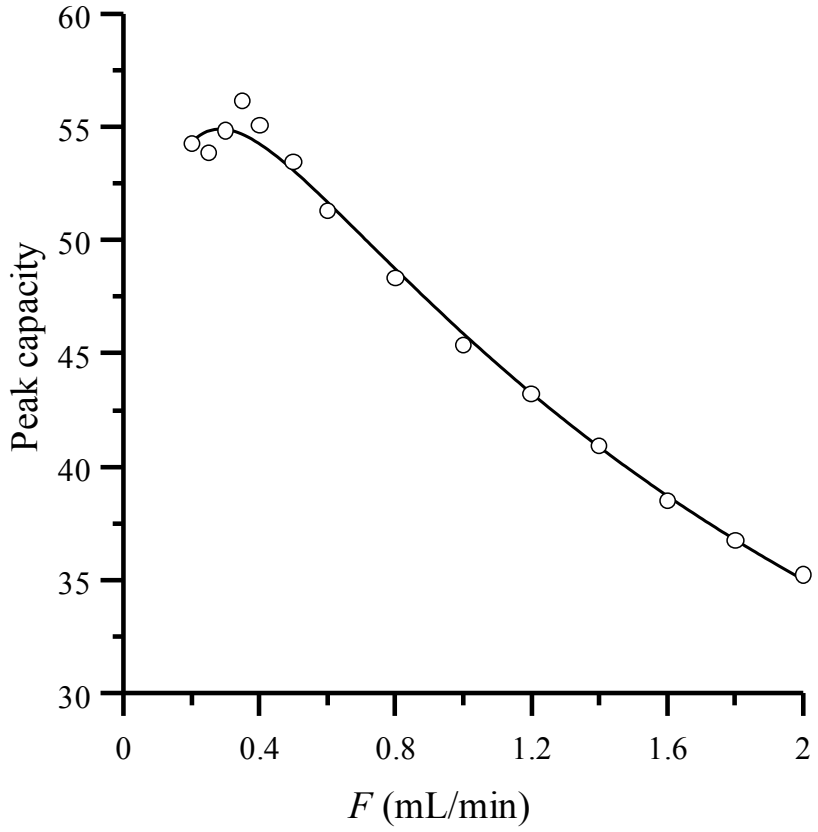

Figure 6. Experimental (circles) and predicted (solid line) peak capacity in the first 20 mL of elution after the dead volume ($V_1 = V_0$ and $V_n = V_0 + 20$), for the Spherisorb column, using the set of sulfonamides as probe compounds.

4. Conclusions

The examination of the behavior at varying flow rates in liquid chromatography indicates that it is possible to predict both the position and shape (width and asymmetry) of chromatographic peaks with high accuracy, with optimization purposes, using the flow rate as the experimental factor. The peak half-widths or widths also allow the characterization of chromatographic columns without the need of measuring the extra-column contributions, which is a source of error in the calculation of the theoretical plate height, especially for compounds with low retention.

The proposed approaches make direct use of the peak half-widths or widths at varying flow rate, for several compounds with similar kinetics and eluted with a selected mobile phase composition, or with several mobile phase compositions, or for a selected compound eluted with several mobile phases. Thus, the effect of the flow rate on the column is described throughout its whole range of elution and not strictly based on the behavior of one compound eluted with a selected mobile phase composition. This may result in more robust, global and significant column parameters. Since there is no need for extra-column measurements, the results are more accurate. Moreover, the study of the asymmetry as a quality factor of the column is possible.

The plots reported in this work are intended to improve the understanding of the column behavior in liquid chromatography and can be considered complementary to the van Deemter plots, as they show the effect of the flow rate on peak asymmetry. They also offer parameters that can be directly used to evaluate the effect of the flow rate on the peak capacity and the resolution with optimization purposes. It should be remarked that the model parameters will depend on the height at which the peak half-widths are measured. We recommend the measurement at 10% peak height, which offers the most informative behavior on peak overlapping, but measurements at any other height are also possible.

Acknowledgements

This work was supported by Project CTQ2013–42558-P (MINECO, Spain).

Author Contributions

Casandra Ortiz-Bolsico: experimental work, peak data measurement and peak data representation. Juan José Baeza-Baeza: project design, experimental design, data interpretation and manuscript revision. María Celia García-Alvarez-Coque: project design and guidance, data interpretation and manuscript writing and revision. All authors read and approved the final manuscript.

Conflicts of Interest

The authors declare no conflict of interest.

References

1. Neue, U.D. *HPLC Columns: Theory, Technology and Practice*; Wiley: New York, NY, USA, 1997.
2. Poole, C.K. *The Essence of Chromatography*; Elsevier: Amsterdam, The Netherlands, 2003.

3. Nawrocki, J. The silanol group and its role in liquid chromatography, *J. Chromatogr. A* **1997**, *779*, 29–71.
4. Bocian, S.; Buszewski, B. Residual silanols at reversed-phase silica in HPLC: A contribution for a better understanding, *J. Sep. Sci.* **2012**, *35*, 1191–1200.
5. Kirkland, J.J.; Yau, W.W.; Stoklosa, H.J.; Dilks, C.H., Jr. Sampling and extra-column effects in high-performance liquid chromatography: Influence of peak skew on plate count calculations. *J. Chromatogr. Sci.* **1977**, *15*, 303–316.
6. Desmet, G.; Clicq, D.; Gzil, P. Geometry-independent plate height representation methods for the direct comparison of the kinetic performance of LC supports with a different size or morphology, *Anal. Chem.* **2005**, *77*, 4058–4070.
7. Baeza-Baeza, J.J.; Pous-Torres, S.; Torres-Lapasió, J.R.; García-Alvarez-Coque, M.C. Approaches to characterise chromatographic column performance based on global parameters accounting for peak broadening and skewness. *J. Chromatogr. A* **2010**, *1217*, 2147–2157.
8. Fekete, S.; Fekete, J. The impact of extra-column band broadening on the chromatographic efficiency of 5 cm long narrow-bore very efficient columns. *J. Chromatogr. A* **2011**, *1218*, 5286–5291.
9. Martin, A.J.P.; Synge, R.L.M. A new form of chromatogram employing two liquid phases, *Biochem. J.* **1941**, *35*, 1358–1368.
10. Baeza-Baeza, J.J.; García-Alvarez-Coque, M.C. A theoretical plate model accounting for slow kinetics in chromatographic elution. *J. Chromatogr. A* **2011**, *1218*, 5166–5174.
11. Fornstedt, T.; Zhong, G.M.; Guiochon, G. Peak tailing and mass-transfer kinetics in linear chromatography. *J. Chromatogr. A* **1996**, *741*, 1–12.
12. Gotmar, G.; Fornstedt, T.; Guiochon, G. Peak tailing and mass transfer kinetics in linear chromatography: Dependence on the column length and the linear velocity of the mobile phase. *J. Chromatogr. A* **1999**, *831*, 17–35.
13. Petersson, P.; Forssen, P.; Edström, L.; Samie, F.; Tatterton, S.; Clarke, A.; Fornstedt, T. Why ultra-high performance liquid chromatography produces more tailing peaks than high performance liquid chromatography, why it does not matter and how it can be addressed. *J. Chromatogr. A* **2011**, *1218*, 6914–6921.
14. Ruiz-Angel, M.J.; Pous-Torres, S.; Carda-Broch, S.; García-Alvarez-Coque, M.C. Performance of different C18 columns in reversed-phase liquid chromatography with hydro-organic and micellar-organic mobile phases. *J. Chromatogr. A* **2014**, *1344*, 76–82.
15. Papadoyannis, I.N.; Zotou, A. Fronting of chromatographic peaks: Causes. In *Encyclopedia of Chromatography*; Cazes, J., Ed.; Marcel Dekker: New York, NY, USA, 2001; pp. 362–363.
16. Ruiz-Angel, M.J.; Carda-Broch, S.; García-Alvarez-Coque, M.C. Peak half-width plots to study the effect of organic solvents on the peak performance of basic drugs in micellar liquid chromatography. *J. Chromatogr. A* **2010**, *1217*, 1786–1798.
17. Baeza-Baeza, J.J.; Ruiz-Angel, M.J.; Carda-Broch, S.; García-Alvarez-Coque, M.C. Half-width plots, a simple tool to predict peak shape, reveal column kinetics and characterise chromatographic columns in liquid chromatography: State of the art and new results. *J. Chromatogr. A* **2013**, *1314*, 142–153.

18. Cabo-Calvet, E.; Ortiz-Bolsico, C.; Baeza-Baeza, J.J.; García-Alvarez-Coque, M.C. Description of the retention and peak profile for Chromolith columns in isocratic and gradient elution using mobile phase composition and flow rate as factors. *Chromatography* **2014**, *1*, 194–210.
19. Baeza-Baeza, J.J.; Ortiz-Bolsico, C.; Torres-Lapasió, J.R.; García-Alvarez-Coque, M.C. Approaches to model the retention and peak profile in linear gradient reversed-phase liquid chromatography. *J. Chromatogr. A* **2013**, *1284*, 28–35.
20. van Deemter, J.J.; Zuiderweg, F.J.; Klinkenberg, A. Longitudinal diffusion and resistance to mass transfer as causes of non-ideality in chromatography. *Chem. Eng. Sc.* **1956**, *5*, 271–289.
21. Torres-Lapasió, J.R. *MICHROM Software*; Marcel Dekker: New York, NY, USA, 2000.
22. García-Alvarez-Coque, M.C.; Torres-Lapasió, J.R.; Baeza-Baeza, J.J. Models and objective functions for the optimisation of selectivity in reversed-phase liquid chromatography. *Anal. Chim. Acta* **2006**, *579*, 125–145.
23. Baeza-Baeza, J.J.; Ortiz-Bolsico, C.; García-Alvarez-Coque, M.C. New approaches based on modified Gaussian models for the prediction of chromatographic peaks. *Anal. Chim. Acta* **2013**, *758*, 36–44.
24. Pous-Torres, S.; Torres-Lapasió, J.R.; Ruiz-Angel, M.J.; García-Alvarez-Coque, M.C. Interpretive optimisation of organic solvent content and flow-rate in the separation of β-blockers with a Chromolith RP-18e column. *J. Sep. Sci.* **2009**, *32*, 2793–2803.
25. Pous-Torres, S.; Baeza-Baeza, J.J.; Torres-Lapasió, J.R.; García-Álvarez-Coque, M.C. Peak capacity estimation in isocratic elution. *J. Chromatogr. A* **2008**, *1205*, 78–89.